

The effect of baroclinicity on the wind profile in the atmospheric boundary layer

R. Floors¹ A. Peña¹ S-E Gryning¹

¹DTU Wind Energy, Risø campus – Department of Wind Energy

Flow center meeting

Outline

1 Introduction

2 Theory

- Barotropic, baroclinic and gradient wind

3 Methodology

- Observations
- WRF simulations

4 Results

- Baroclinic wind profile
- Turning of the wind

5 Conclusions

Outline

- Should we account for baroclinicity when looking at 'tall' profiles?
- Meteorological masts usually not high enough to investigate large-scale effects, but now we have long-term measurements from longe-range wind lidar
- WRF analysis simulations to get large-scale parameters from both locations for two years.

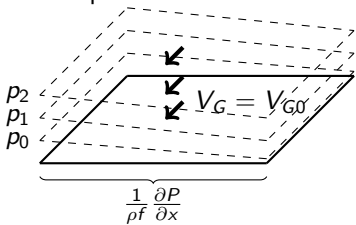
Barotropic and baroclinic flow in homogeneous, stationary PBL

- $\frac{\partial}{\partial z} \overline{u'w'} = -\frac{1}{\rho} \frac{\partial P}{\partial x} + fV,$
 $\frac{\partial}{\partial z} \overline{v'w'} = -\frac{1}{\rho} \frac{\partial P}{\partial y} - fU$

Barotropic and baroclinic flow in homogeneous, stationary PBL

- $\frac{\partial}{\partial z} \overline{u'w'} = -\frac{1}{\rho} \frac{\partial P}{\partial x} + fV,$
 $\frac{\partial}{\partial z} \overline{v'w'} = -\frac{1}{\rho} \frac{\partial P}{\partial y} - fU$
- $U_G = -\frac{1}{\rho f} \frac{\partial P}{\partial y}, V_G = \frac{1}{\rho f} \frac{\partial P}{\partial x}$

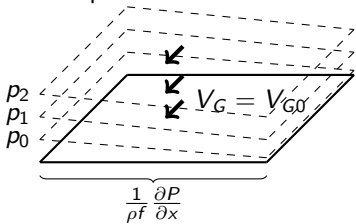
Barotropic



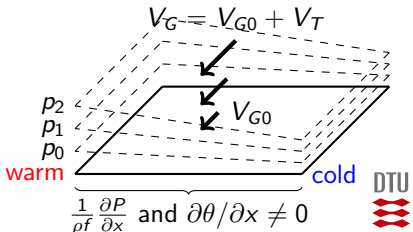
Barotropic and baroclinic flow in homogeneous, stationary PBL

- $\frac{\partial}{\partial z} \overline{u'w'} = -\frac{1}{\rho} \frac{\partial P}{\partial x} + fV$,
 $\frac{\partial}{\partial z} \overline{v'w'} = -\frac{1}{\rho} \frac{\partial P}{\partial y} - fU$
- $U_G = -\frac{1}{\rho f} \frac{\partial P}{\partial y}$, $V_G = \frac{1}{\rho f} \frac{\partial P}{\partial x}$
- $U_T = -\frac{1}{f} \frac{\partial(\Phi_{z2} - \Phi_{z1})}{\partial y}$, $V_T = \frac{1}{f} \frac{\partial(\Phi_{z2} - \Phi_{z1})}{\partial x}$

Barotropic



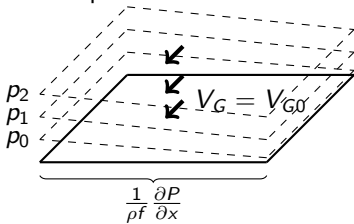
Baroclinic



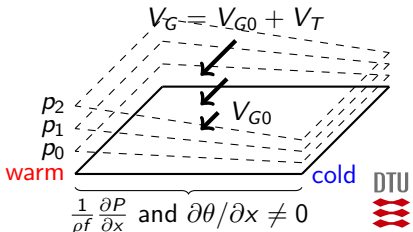
Barotropic and baroclinic flow in homogeneous, stationary PBL

- $\frac{\partial}{\partial z} \overline{u'w'} = -\frac{1}{\rho} \frac{\partial P}{\partial x} + fV$,
 $\frac{\partial}{\partial z} \overline{v'w'} = -\frac{1}{\rho} \frac{\partial P}{\partial y} - fU$
- $U_G = -\frac{1}{\rho f} \frac{\partial P}{\partial y}$, $V_G = \frac{1}{\rho f} \frac{\partial P}{\partial x}$
- $U_T = -\frac{1}{f} \frac{\partial(\Phi_{z2} - \Phi_{z1})}{\partial y}$, $V_T = \frac{1}{f} \frac{\partial(\Phi_{z2} - \Phi_{z1})}{\partial x}$
- $U_G = U_{G0} + U_T$, $V_G = V_{G0} + V_T$

Barotropic



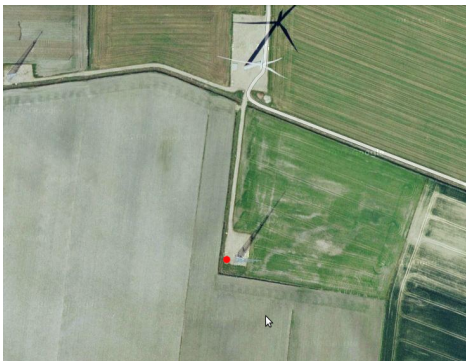
Baroclinic



Measurements Høvsøre

Observations

Data source	Heights [m]
Cup	10, 40, 60, 80, 100
Sonic	10, 100
Lidar	100 – 2000 (50 m interval)



Measurements Høvsøre

Observations

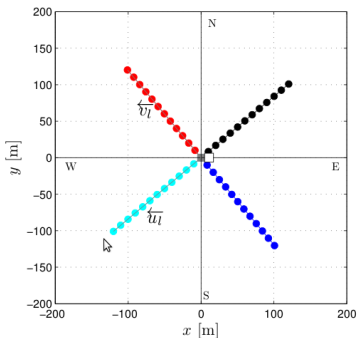
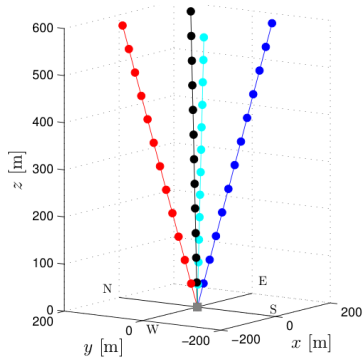
Data source	Heights [m]
Cup	10, 40, 60, 80, 100
Sonic	10, 100
Lidar	100 – 2000 (50 m interval)



Measurements Høvsøre

Observations

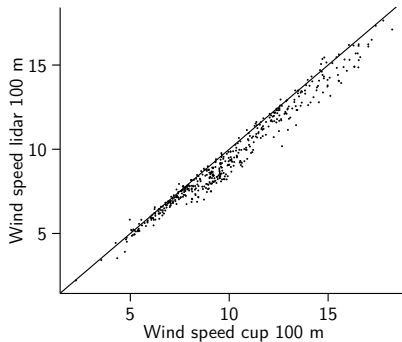
Data source	Heights [m]
Cup	10, 40, 60, 80, 100
Sonic	10, 100
Lidar	100 – 2000 (50 m interval)



Measurements Høvsøre

Observations

Data source	Heights [m]
Cup	10, 40, 60, 80, 100
Sonic	10, 100
Lidar	100 – 2000 (50 m interval)



Measurements Hamburg

Observations

Data source	Heights [m]
Sonic	10 (small mast), 50, 110, 175, 250 (big mast)
Lidar	100 – 2000 (50 m interval)
Radiosondes	0 – 4000 (averaged into 50 m interval)



Measurements Hamburg

Observations

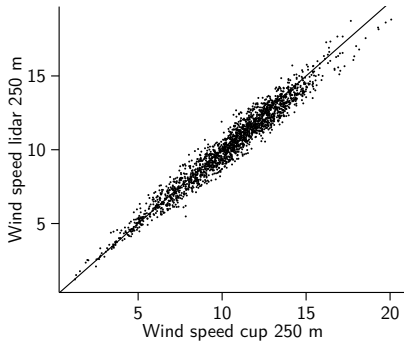
Data source	Heights [m]
Sonic	10 (small mast), 50, 110, 175, 250 (big mast)
Lidar	100 – 2000 (50 m interval)
Radiosondes	0 – 4000 (averaged into 50 m interval)



Measurements Hamburg

Observations

Data source	Heights [m]
Sonic	10 (small mast), 50, 110, 175, 250 (big mast)
Lidar	100 – 2000 (50 m interval)
Radiosondes	0 – 4000 (averaged into 50 m interval)

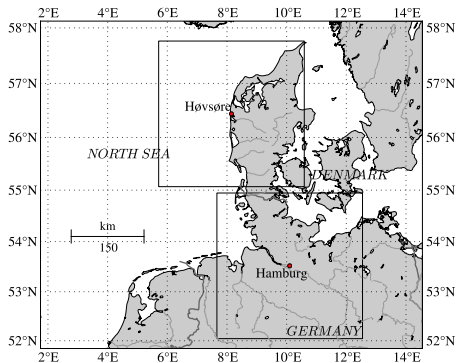


WRF V3.4 setup

- YSU (first order): $\overline{u'w'} = -K_m \left(\frac{\partial U}{\partial z} - \gamma_m \right) - \overline{u'w'} h \left(\frac{z}{h} \right)^3$
- NOAH land surface
- Thompson microphysics scheme,
- RRTM long-wave radiation
- Dudhia short-wave radiation

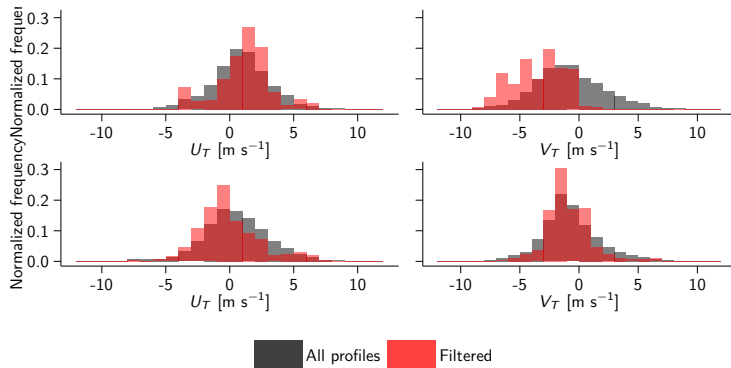
- WRF simulations 1 april 2010 – 1 april 2010 (Høvsøre)
- WRF simulations 1 april 2011 – 1 april 2012 (Hamburg)
- 10 day 'analysis' simulations, 1 day spin-up
- Boundary conditions NCEP FNL Analysis, global sea-surface temperature analysis NCEP
- Nudging above 10th model level in outermost domain

Grid boxes for deriving gradients



- Used grid box from WRF simulations, 18 and 6 km hor. res.
- U_{G0} and V_{G0} account for curvature of the isobars in this area

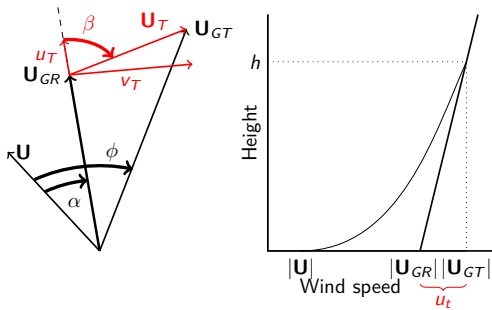
Is the influence of thermal wind significant?



Distributions thermal wind at 950 m in Høvsøre (top) and Hamburg (bottom)



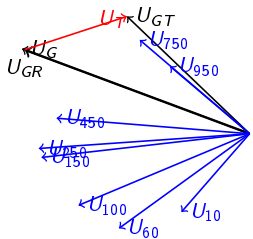
Baroclinic wind profile: in theory



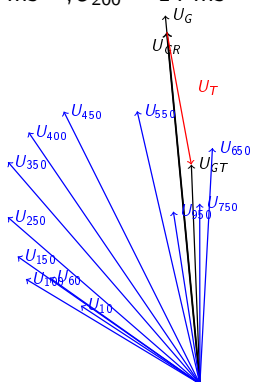
Wind vectors looking down the PBL; Wind profile positive geostrophic shear;

Baroclinic wind profile: in practice

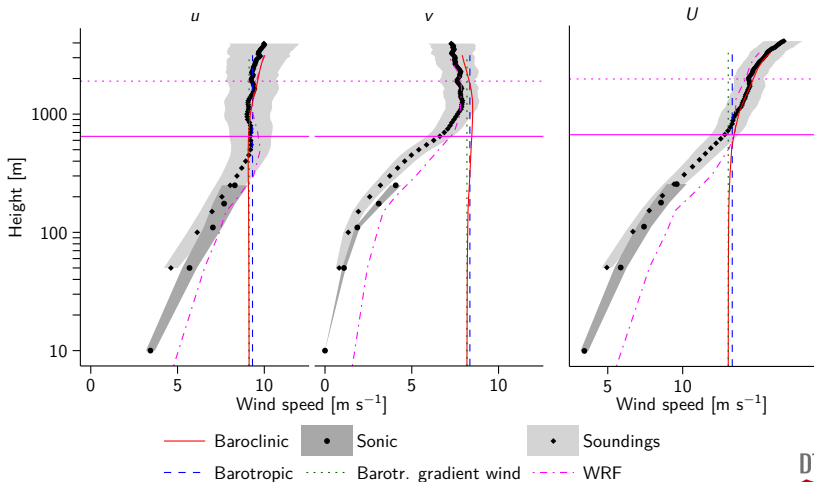
High wind veer, $U = 10 \text{ ms}^{-1}$



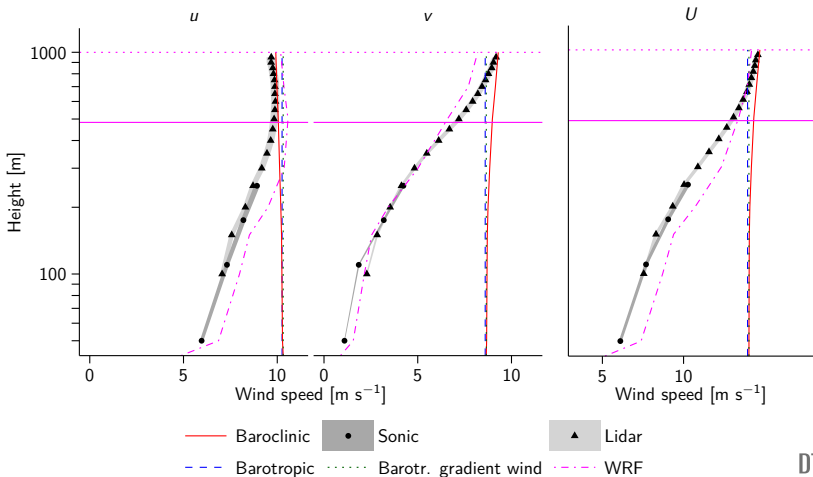
High wind shear, $U_{10} = 7 \text{ ms}^{-1}$, $U_{200} = 14 \text{ ms}^{-1}$



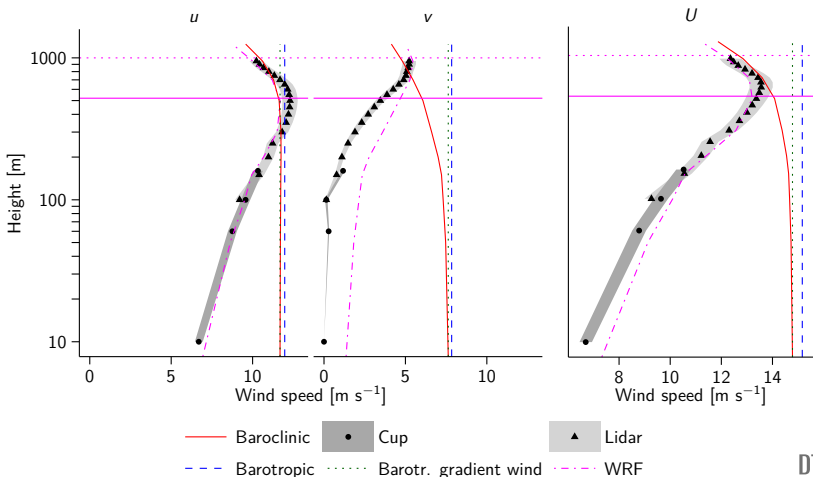
Long-term mean wind profile – radiosondes



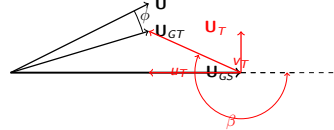
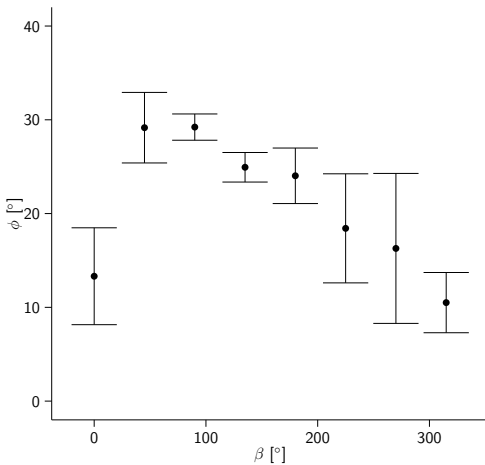
Long-term mean wind profile – Hamburg (rural and urban sector)



Long-term mean wind profile – Høvsøre (easterly sector)



Turning of the wind with height



Geostrophic drag law

$$U_G = \frac{u_{*0}}{k} \sqrt{(\ln(u_{*0}/fz_0) - A)^2 + B^2}, A \approx 1.3, B \approx 4.4$$

TABLE A.I

List of field experiments giving the values of A and B : Middle and higher latitudes.

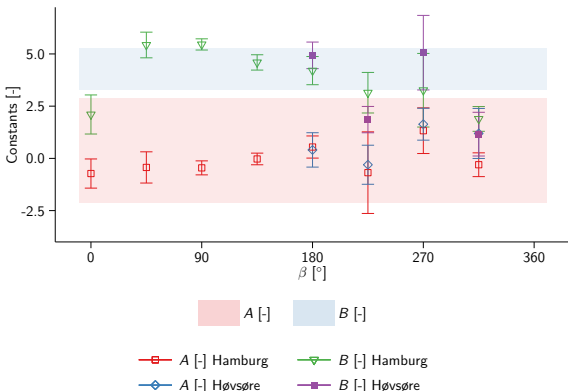
Experiment	Latitude	t_0	G	Lat	Re	u_{*0}/G	a_0	A	B	Reference
Pri-Wangara	-34.5	0.0005	13.7	7.5	0.030	19	0.9	4.5		Clarke and Hines (1973); Dacon (1973)
Wangara	-34.5	0.0035	13.9	7.7	0.029	18	1.1	4.3		Clarke and Hines (1974)
Sangamon	39.5	0.13	7.7	5.8	0.034	26	0.8	4.7		Hicks et al. (1981) ^{a,d}
Rush	39.6	0.098	12.8	6.1	0.034	25	0.3	5.0		Sisterson et al. (1983) ^{a,d}
DeWitt	40.2	0.17	11.4	5.9	0.037	28	1.2	5.0		Coulier et al. (1984) ^{a,d}
O'Neill	42.5	0.009	14.5	7.2	0.033	22.6	2.2	4.6		Walmsley (1992)
Lakewood	45.2	1.40	14.1	5.0	0.052	37	2.5	4.7		Johnson (1965); Dacon (1973)
Ellendale	46.1	0.023	10.6	6.6	0.034	19	0.8	3.8		Cunady (1967); Johnson (1962); Gregg (1922)
Voves	48.4	0.098	6.2	5.8	0.040	25	1.0	4.3		Bilfield et al. (1981); Andre and Lacambre (1981)
Upson	51.3	0.006	12.4	7.3	0.029	20.6	0.4	4.8		Walmsley (1992) ^a
Leipzig	51.4	0.14	17.5	6.0	0.037	26	0.9	4.7		Lettau (1980); Möldner (1932) ^b
German Bight I	54	0.00015	14.6	8.9	0.025	13.5	1.4	3.7		Hase (1974) ^b
German Bight II	54									2.6 3.4 Lüthardt and Hase (1981) ^b
KONTUR	55	0.00028	18.6	8.9	0.027	13	2.4	3.5		Grant and Whitelord (1987) ^c
Kiel Bight	55	0.0001	14.3	9.1	0.022	16.5	-0.1	5.1		Hase and Dunkel (1974) ^a
North Sea	56	0.00029	21.0	8.8	0.024	17	0.6	4.8		Gill (1967) ^c
North Atlantic	56	0.0001	11.0	6.0	0.027	17	2.9	4.3		Dacon (1973) ^a
Obninsk	56				6.4	0.036		1.5	5.5	Dacon (1973)
Viseikino	60				6.0	30				
JASIN	60	0.00008	10.3	8.6	0.028	16	1.4	4.2		Nicholls (1985)
AIRTEX	75	0.0035	12.0	7.4	0.033	21	2.3	4.4		Brown (1981) ^b

^aCalculations made by present authors, or adjustments made to published values.^bMay have partially overlapping data set with German Bight I.^cScaling height may have been determined by the inversion height, rather than $u_{*0}/(fz)$.^dLimited data in near-neutral conditions.

Average values from Table A.I.

 $A = 1.3 \pm 0.2$. $B = 4.4 \pm 0.1$.

Geostrophic drag law



Conclusions

- Barotropic PBL is an exception, not the rule
- Taking into account baroclinicity improves agreement with estimated wind speed at PBL top compared to observations
- Baroclinicity largest for easterly sector for Hovsore, also sondes and hamburg lidar baroclinic
- Turning of the wind and normalized stress profiles often influenced by baroclinicity
- Not taking into account baroclinicity can explain part of scatter in A and B